Ab Initio Kinetics of Gas Phase Decomposition Reactions

Onise Sharia and Maija M. Kuklja*

Department of Materials Science and Engineering, University of Maryland, College Park, Maryland 20742, United States

Received: August 25, 2010; Revised Manuscript Received: October 13, 2010

The thermal and kinetic aspects of gas phase decomposition reactions can be extremely complex due to a large number of parameters, a variety of possible intermediates, and an overlap in thermal decomposition traces. The experimental determination of the activation energies is particularly difficult when several possible reaction pathways coexist in the thermal decomposition. Ab initio calculations intended to provide an interpretation of the experiment are often of little help if they produce only the activation barriers and ignore the kinetics of the decomposition process. To overcome this ambiguity, a theoretical study of a complete picture of gas phase thermo-decomposition, including reaction energies, activation barriers, and reaction rates, is illustrated with the example of the β-octahydro-1,3,5,7-tetranitro-1,3,5,7-tetrazocine (HMX) molecule by means of quantum-chemical calculations. We study three types of major decomposition reactions characteristic of nitramines: the HONO elimination, the NONO rearrangement, and the $N-NO_2$ homolysis. The reaction rates were determined using the conventional transition state theory for the HONO and NONO decompositions and the variational transition state theory for the $N-NO_2$ homolysis. Our calculations show that the HMX decomposition process is more complex than it was previously believed to be and is defined by a combination of reactions at any given temperature. At all temperatures, the direct $N-NO_2$ homolysis prevails with the activation barrier at 38.1 kcal/mol. The nitro−nitrite isomerization and the HONO elimination, with the activation barriers at 46.3 and 39.4 kcal/mol, respectively, are slow reactions at all temperatures. The obtained conclusions provide a consistent interpretation for the reported experimental data.

I. Introduction

The understanding of the thermal and kinetic aspects of gas phase decomposition reactions is imperative in many fundamental and applied fields, including the environmental sciences, combustion and explosions, catalysis, matter under extreme condition, and planetary sciences. Obtaining reliable data to describe thermochemistry and kinetics can be extremely complex for large molecules due to a large number of parameters, a variety of possible intermediates, and an overlap in the thermal decomposition traces of parallel processes. The experimental determination of the activation energies is particularly difficult when several possible reaction pathways coexist in the course of the thermal decomposition. Ab initio quantum-chemical calculations aimed to provide an interpretation of the experiment are often of little help if they produce only activation barriers and ignore the kinetics of the decomposition process. Although the theoretical methods to overcome this ambiguity do exist, their application is far from trivial, especially for large molecules and fast or complex decomposition processes.

For this theoretical study of a complete picture of gas phase thermo-decomposition, including reaction energies, activation barriers, and reaction rates, we selected an illustrative example of the β-octahydro-1,3,5,7-tetranitro-1,3,5,7-tetrazocine (β-HMX) molecule. We think it serves as an ideal model system for the task for several reasons. First, a β-HMX molecule is big and complex and contains functional chemical groups typical for a wide class of nitro-compound materials. Second, despite concerted efforts to extensively study its decomposition process, elucidation of the primary and secondary dissociation mechanisms remains a challenge for both experimental[1−3] and theoretical exploration.[4−6] In experiments, it is difficult to distinguish between competing chemical reactions during the initial steps of the rapid decomposition of HMX as a global decomposition is measured. One has to speculate from the global kinetics and reaction products which reactions are taking place. As a result, the reported decomposition barriers vary by a factor of 2−3 and the pre-exponential factors in the reaction rates differ by orders of magnitude. More so, even the first step in the decomposition process is still a subject of debate. In addition, HMX is an important high energy density material for a broad range of technological applications spanning from high explosives and propellants to rocket engine fuels. Finally, as will be shown below, the decomposition process of HMX is composed of several seemingly coexisting pathways with a fairly small difference in activation barriers and significantly different nature of corresponding bond dissociation processes. The hydrogen transfer and nitro-to-nitrite isomerization reactions possess well-defined transition sates while the direct $N-NO_2$ bond homolysis proceeds as a reaction with no activation barrier.

In this article, we will show that theoretical calculations of both activation barriers and reaction rates for each possible chemical reaction and their careful analysis are crucial in understanding the decomposition mechanisms and interpreting experiments. In addition to activation barriers that are traditionally reliably delivered by density functional theory, we apply conventional transition state theory (CTST)[7] and variational transition state theory (VTST)[8] to analyze an interplay among three main decomposition reactions in HMX: direct $N-NO_2$ homolysis, hydrogen transfer with the consequent HONO elimination, and nitro−nitrite isomerization (NONO rearrangement) with the consequent NO elimination. The obtained conclusions regarding the chemical decomposition mechanisms and the conditions under which the dominating reactions proceed,

10.1021/jp108065c
Published on Web 11/15/2010

are discussed and interpreted in conjunction with the available experimental data.

II. Method of Calculations

A conventional transition state theory has been discussed widely in the literature.[7] Within this theory, the transition rate is given by

$$k = \frac{\langle \delta(x - x^{TS})\theta(\dot{x})\rangle}{\langle \theta(x^{TS})\rangle} \quad (1)$$

where x is a reaction coordinate, x^{TS} is a transition point, θ is a step function, and the brackets indicate averaging over an ensemble. This equation can be straightforwardly applied when there is a clearly defined transition state for a reaction, assuming vibrational and rotational variables are separable. Integrating eq 1 over these variables and taking into account only harmonic terms, it becomes[9]

$$k = \frac{k_B T}{h}\frac{Z_{vib}^{TS}}{Z_{vib}^{0}}\frac{Z_{rot}^{TS}}{Z_{rot}^{TS}}\exp(-\beta E_B) \quad (2)$$

Here, k_B is the Boltzmann constant, T is the temperature of the system, h is Plank's constant, Z_{vib}^{0} is the vibrational partition function of the initial system, Z_{vib}^{TS} is the vibrational partition function of the system at the transition point, Z_{rot}^{0} is the rotational partition function of the initial system, Z_{rot}^{TS} is the rotational partition function of the system at the transition point, β is equal to $1/k_B T$ and E_B is the barrier height of the reaction, obtained as the difference between the total energy of the initial system and the system at the transition point. The vibrational partition function can be written as[10]

$$Z_{vib} = \prod_{i=1}^{M}\frac{\exp(-\beta\hbar\omega_i/2)}{1 - \exp(-\beta\hbar\omega_i)} \quad (3)$$

where M is the number of vibrational modes with frequencies ω_i. For the molecule in the initial system, the number of vibrational modes is $3N - 6$, where N is the number of atoms, and becomes $3N - 7$ at the transition state as one vibrational mode becomes negative. In this equation, a quantization of vibrations is taken into account. The quantization is important mainly because of the numerator in eq 3 and the quantum nature of zero point energy corrections; it corresponds to the zero point energy of vibrations, which is not present in the classical limit. We will show below that the zero point energy reduces the energy barrier of the reaction. For the rotational partition function, the quantization is not important. The classical rotational partition function is given by[11]

$$Z_{rot} = \frac{8\pi}{h^3}(I_1 I_2 I_3)^{1/2}\left(\frac{2\pi}{\beta}\right)^{3/2} \quad (4)$$

were I_1, I_2, and I_3 are moments of inertia along the principal axes. We note that the sizes of HONO and NONO are significantly smaller than the size of the HMX molecule. Therefore, the moments of inertia of the initial system and the system at the transition state can be considered almost the same. This approximation will allow us to ignore rotations for the reactions of interest.

For the $N-NO_2$ homolysis reaction, which does not exhibit a well-defined transition state during the decomposition process, we use variational TST.[8] Within VTST, one has to calculate the rate constant as a function of x^{TS} and find its minimum. In the equilibrium state, when an NO_2 group is attached to an HMX molecule, it has nine vibrational modes. However, after splitting from the molecule, the nitro group loses six vibrational modes and gains three rotational and three translational modes. An important assumption we make here is that the interaction energy between NO_2 and the remaining HMX molecule (which is essentially the $N-NO_2$ bond energy) depends only on the distance between HMX and the center of mass of NO_2 and not on an orientation of the NO_2 moiety. We will illustrate that this assumption is correct to a good approximation (vide infra). This allows us to choose the $N-NO_2$ bond distance as a reaction coordinate, meaning that the translational and rotational degrees of freedom of NO_2 are independent of each other. Overall, for the $N-NO_2$ fission reaction, there are three types of independent degrees of freedom: (1) $3N - 12$ atomic vibrational modes, (2) three NO_2 rotational modes, and (3) three NO_2 translational modes. Since the reaction coordinate depends only on the position of the center of mass of the NO_2 moiety, we can take an average over the rotational and vibrational coordinates and momenta in eq 1:

$$k = \frac{Z_{rot}^{NO_2} Z_{vib}^{TS}}{h^3 Z_{vib}^{0}}\int d^3\vec{P}\, d^3\vec{R}\,\theta(\dot{x})\,\dot{x}\delta(x - x^{TS}) \times \exp\left(-\beta\left(\frac{P_1^{\,2} + P_2^{\,2} + P_3^{\,2}}{2m_{NO_2}} + V(R_1, R_2, R_3)\right)\right) \quad (5)$$

where $\vec{P}$ and $\vec{R}$ are the center of mass momentum and the coordinate of the NO_2 molecule, respectively. The term $V(R_1,R_2,R_3)$ describes a change of the total energy of the system, which is a change of the $N-NO_2$ bond energy, and x represents the bond energy as a function of the geometry of the system. For $\dot{x}$ we obtain

$$\dot{x} = \frac{d}{dt}V = \vec{\nabla}V\cdot\frac{d}{dt}\vec{R} = |\vec{\nabla}V|\dot{R}_\perp \quad (6)$$

where $\dot{R}_\perp$ is a component of $\dot{\vec{R}}$ perpendicular to the $V = E_B$ surface. It can be written as $P_\perp/2m_{NO_2}$. Using the property of the delta function

$$\int d^3R\,\delta(V(\vec{R}) - E_B)f(\vec{R}) = \int_{V=E_B} d\sigma\,\frac{f(\vec{R})}{|\vec{\nabla}_R V|} \quad (7)$$

and integrating over $\vec{P}$ and $\vec{R}$ in eq 5, we obtain

$$k = \frac{Z_{rot}^{NO_2} Z_{vib}^{TS}}{h^3 Z_{vib}^{0}}\frac{2m_{NO_2}\pi\sigma}{\beta^2}\exp(-\beta E_B) \quad (8)$$

where σ is the area of the surface defined by the $V = E_B$. Next, we need to find σ and to determine the value of E_B for which the rate becomes minimal as follows from VTST.

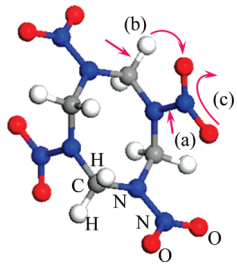

Figure 1. Structure of an HMX molecule and three possible primary decomposition reactions. The direct N−NO_2 homolysis (a) is simulated by the elongation of the N−N bond, the HONO elimination (b) is demonstrated as switching of the C−H---O bond to C---H−O bond, and the nitro−nitrite isomerization (c) is displayed by a combined rotation of the NO_2 group and the elongation of the N−N bond to form NONO.

In the calculations, we used plane wave density functional theory[12,13] in the GGA approximation with the PBE functional[14] and the PAW[15] method as implemented in the VASP[16−19] code. The kinetic energy cutoff was set to 600 eV. Atomic positions were relaxed using conjugate gradient and quasi-Newtonian methods within a force tolerance of 0.05 Å/eV.

III. Reaction Energies, Activation Barriers, and Kinetics

We model a gas phase HMX by placing a single β-HMX molecule in a 15 × 15 × 15 $Å^3$ cell and optimizing the atomic positions with the VASP code. Calculations are performed only at the Gamma point. By using this model, we consider three chemical bond dissociation reactions as candidates for the initial step in the overall decomposition process: the hydrogen transfer with HONO elimination,[2,4,20] the nitro−nitrite isomerization (NONO rearrangement) with NO elimination,[21] and the direct N−NO_2 homolysis[2,4,20] as illustrated in Figure 1. The HONO elimination is modeled by transferring one H atom to the axial NO_2 and relaxing the atomic positions. To simulate the NONO rearrangement, we extend the axial N−NO_2 bond and slightly rotate NO_2. After the relaxation, one of the O atoms from the NO_2 group binds with an N atom from the ring, forming NONO. In the third reaction, the N−NO_2 homolysis is modeled by moving the NO_2 group away along the N−NO_2 bond direction by 5.7 Å. The N-NO_2 homolysis was studied in both spin-polarized and spin-nonpolarized computational schemes. The reaction energies of the HONO elimination, the NONO rearrangement, and the N−NO_2 homolysis are found by taking the differences of the total energies of the equilibrium HMX molecule and of the corresponding final state (HONO, NONO, or split-off NO_2). All three reactions are established to be endothermic with the energies of 2.42, 19.23, 57.81 (triplet), and 42.84 (singlet) kcal/mol, respectively (see Figure 2a−c and Table 1).

The minimal energy paths of the reactions and the corresponding transition states were determined by means of the climbing nudged elastic band method.[22] We calculated six intermediate images between the initial and final atomic configurations. The activation barriers are defined as the differences between the total energies of the equilibrium HMX molecule and the corresponding transition states in the course of the bond dissociation. The obtained activation energies of the HONO and NONO reactions are found to be 44.59 and 49.46 kcal/mol (Figure 2a,b), respectively. The N−NO_2 homolysis pathway does not have a saddle point (Figure 2c); thus, the activation barrier is considered to be the same as the reaction energy. More details of these and some additional reaction pathways and the transition state geometry configurations will be given elsewhere.[23]

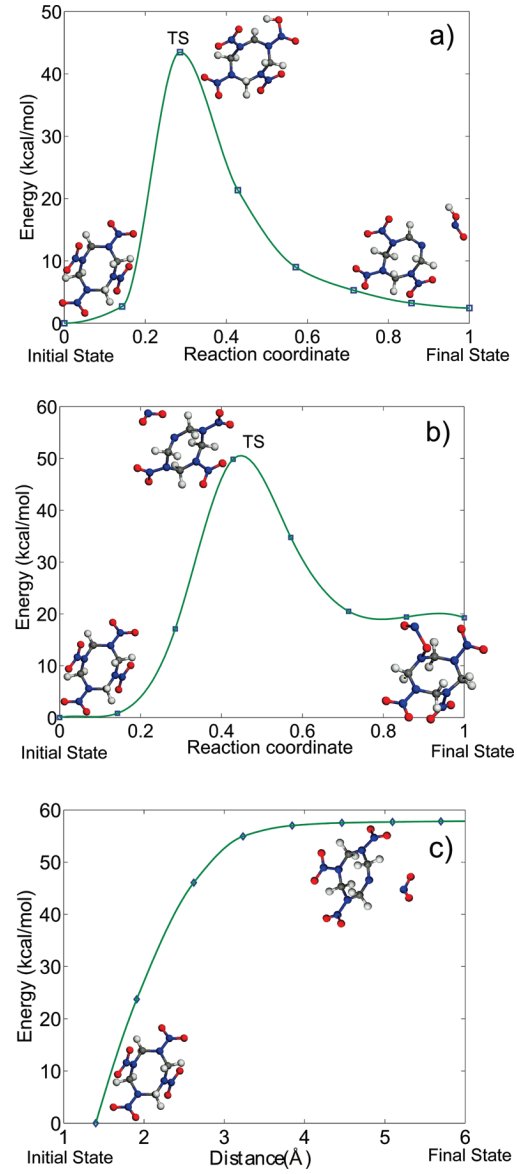

Figure 2. Minimal energy pathway for the dissociation reactions: (a) HONO elimination; (b) NONO rearrangement (c) N−NO_2 dissociation (the singlet state is shown). TS stands for the transition state.

TABLE 1: Reaction Energies, Barriers and Rates for HONO Elimination, NONO Rearrangement, and N−NO_2 Homolysis as Primary Candidates for the Initial Step in the Endothermic Decomposition of HMX[a]

reaction	reaction energy (kcal/mol)	E_B (kcal/mol)	ln(A (s^{-1}))	ln(A (s^{-1})) from eq 9
HONO elimination	2.4	39.4	32.9	32.5
NONO isomerization	19.2	45.8	34.2	38.4
N−NO_2 homolysis (singlet)	57.8	52.3	43.7	44.8
N−NO_2 homolysis (triplet)	42.8	38.1	41.3	31.2

[a] Barrier heights include zero point energy corrections.

In applying VTST to properly describe the kinetics of the N−NO_2 homolysis reaction, we need to determine the energy profile of the N−NO_2 bond dissociation and determine the isoenergetic surfaces (eq 8) (a constant energy surface area as

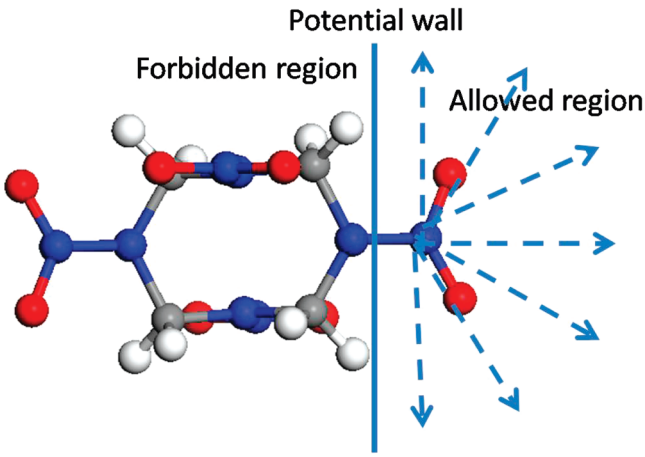

Figure 3. Allowed directions of the dissociation pathways for the N−NO_2 homolysis reaction (shown with dashed arrows).

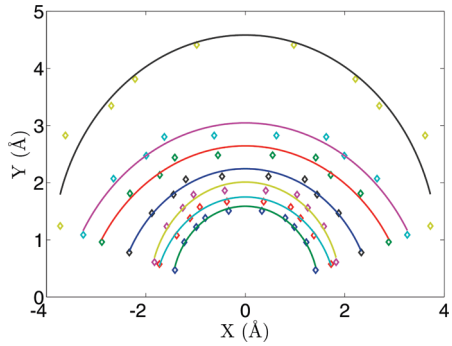

Figure 4. Projection of constant energy surfaces on a plane for energies 10, 20, 30, 40, 50, 55, and 57.5 kcal/mol. The "diamonds" indicate the results of ab initio calculations. The solid lines represent a fit to a circle. Actual calculations were performed only for positive X, and points for negative X are extrapolated on the basis of the symmetry of the molecule.

a function of the N−NO_2 bond energy). In general, this is a difficult task. However, for our system, a derivation of the shape of the isoenergetic surfaces happened to be fairly simple. Before defining the surface shape and its area, we will illustrate that a fairly rough approximation works well here because we are interested in the logarithmic value of the transition rate and, therefore, for the prefactor of k (eq 7), a lesser accuracy than is necessary for the exponential term, E_B, would be sufficient. For example, assuming the error in determining the surface area is as large as 100% (note that our estimate is much better), the corresponding error of its logarithm will be only about 1.3%.[24]

Now, we will use simple speculations to demonstrate that the constant energy surfaces may be well represented by semispheres. The tips we used here are likely to be valid for an arbitrary large molecule. One can imagine that once NO_2 is split off from the HMX molecule, it will move away easily while if pushed toward the rest of the HMX molecule, it will encounter a potential wall without penetration. Figure 3 displays the allowed dissociation pathways with the dashed arrows and the forbidden region for NO_2 movements with the solid line. Indeed, in calculating the minimal energy paths for the N−NO_2 homolysis in the allowed directions, we found that the constant energy surfaces are very close to semispherical shapes. In Figure 4, we show the isosurfaces projected on one of the planes. Thus, the area of the constant energy surface can be taken as $\sigma = 3\pi R^2$. From this, we deduce that the transition rate increases quadratically with the increase of the N−NO_2 bond length. To determine the value of R for which the rate constant is minimal,

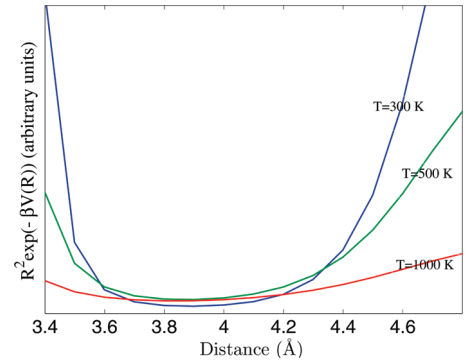

Figure 5. Rate constants (multiplied by an arbitrary number) as a function of R.

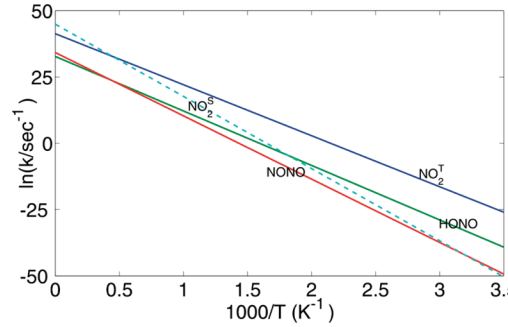

Figure 6. Reaction rates as a function of temperature. NO_2^S denotes the singlet state and NO_2^T denotes the triplet state of the dissociated system.

we plot $R^2 \exp(-V(R)/k_BT)$ as a function of R and determine that its transition point corresponds to the range of distances from 3.8 to 3.9 Å depending on temperature (Figure 5). Now, one can find the needed bond energy E_B to substitute in eq 8 by matching the range 3.8−3.9 Å, found from Figure 5, to the total energy as a function of N−NO_2 bond distance in Figure 2. One can see that the bond energy $V(R)$ at 3.8 Å is almost the same as the N−NO_2 formation energy. By doing this, we assign this point in Figure 2 to be considered now as a transition state for N−NO_2 dissociation.

Further, we explore our earlier assumption that the bond energy at the transition point is independent of the orientation of the NO_2 molecule. By probing a set of different molecular orientations, we find that the resultant energy variations are within 1 kcal/mol.

Next, we calculate the vibrational frequencies for all of the considered structures by DFT perturbation theory:[25] the perfect HMX molecule, the HONO configuration at the transition point, the NONO isomer at the transition point, and the N−NO_2 homolysis. Furthermore, we derive the moments of inertia of an NO_2 molecule along the principal axes,[26] which are 3.717×10^{-47}, 6.599×10^{-46}, and 6.858×10^{-46} kg·m^2 along x, y, and z, respectively.

Finally, the reaction rates are determined using eq 2 for the HONO and NONO reactions and eq 8 for the N−NO_2 homolysis. The obtained activation barriers (including zero point energy corrections) and Arrhenius factors are collected in Table 1. Figure 6 shows the logarithmic dependence of k on 1000/T. As can be seen, at low temperatures, the hydrogen transfer mechanism has the activation barrier at 39.4 kcal/mol, very close to the N-NO_2 activation barrier, indicating that the HONO elimination could be among the earliest decomposition reactions in HMX. However, it is also a fairly slow reaction, which is reflected in its smallest reaction constant at 32.9 s^{-1}, implying

that it can be quickly overstepped by another faster reaction. At all temperatures the $N-NO_2$ homolysis prevails in the decomposition; its activation barrier is the lowest among the reactions probed here at 38.1 kcal/mol and its reaction constant is large at 41.3 s^{-1}. The nitro−nitrite isomerization, NONO, with the activation barrier at 45.8 kcal/mol and the reaction constant at 34.2 s^{-1}, is the slow process at all temperatures. This suggests that the NO elimination hardly contributes to the initiation of the decomposition of HMX, being always only a secondary reaction, which may proceed on the background of the primary decomposition mechanisms. The obtained here results are consistent with previous theoretical studies, which also found that $N-NO_2$ homolysis is the dominating reaction at low temperatures[4] and the fastest at above 400 K.[27] Another study also found that the $N-NO_2$ is the dominating reaction under very high temperatures.[28]

Now, we will try to link our results to the experiment and attempt to explain a fair amount of the dispersion in the experimental values that have reported the activation barriers for gas phase HMX from 32 to 53 kcal/mol and reaction constants from 28 to 47 at 205−383 °C.[29] The discrepancies observed in the global kinetic measurements of the thermal decomposition of HMX were attributed to the history and characteristics of the samples, variations in the experimental conditions,[29] different heating rates, and the potentially strong effects of autocatalytic reactions.[30] It is also known that clustering of HMX molecules occurs in the gas phase, even at low pressure,[31] so it was even proposed that isolated molecules are probably not decomposing.[29] Naturally, one has to keep in mind that the measurements reflect the rate of the overall decomposition process as opposed to a specific reaction as simulated in this study. Although experimental values of the HMX decomposition rates and activation barriers range widely, most data were noted to exhibit a linear relation between ln A and E_B:[29]

$$\ln(A\ (s^{-1})) = 0.96E_B\ (\text{kcal/mol}) - 5.4 \qquad (9)$$

This relationship, sometimes called the kinetic compensation effect,[32] was suggested to account for and unify most of the differences in the reported rates.[29] To check whether the regression holds for the individual reactions and also to validate our calculations, we added the values of ln A determined from eq 9 corresponding to our calculated values of E_B to Table 1 and compared them to the reaction constants calculated here from DFT. Our calculated Arrhenius factors for the HONO elimination (32.9) and the singlet state $N-NO_2$ homolysis (43.7) turned out to be in remarkable agreement with eq 9, which yields 32.5 and 44.8, respectively. The triplet state $N-NO_2$ homolysis' constant (41.3) and the NONO rearrangement's constant (34.2) deviate more than the other two reaction constants from the experimental data. Overall following our results, the activation barriers for both the HONO elimination (39.4 kcal/mol) and the $N-NO_2$ fission (38.1 kcal/mol) reactions fall in the experimentally observed range[33] of activation barriers at 32-53 kcal/mol.[29] Similarly, the calculated reaction rate constants for the HONO (32.9) and the $N-NO_2$ (41.3) dissociation mechanisms are also found to be within the experimentally measured range at 28-47 s^{-2}.[29] At the same time, the obtained conclusions regarding the trends in the relationship between the reaction constant and the activation barrier for the individual reactions fall short in supporting the chemical compensation effect.

IV. Summary and Conclusions

We applied a combination of quantum chemistry and the theory of transition states in its standard and variational versions to simulate the entire process of gas phase thermochesmitry, including understanding the nature of potential decomposition mechanisms at the earliest stages and deriving the corresponding reaction energies, activation barriers, and the reaction rates. We illustrate the approach used on an example of a large and complex organic molecule, HMX. We calculate the reaction rates for the major decomposition mechanisms of gas phase HMX, the direct $N-NO_2$ fission, and the HONO and NONO isomerizations. It was established that the decomposition process in HMX is complex and may be determined by a competition of at least two chemical reactions, with a visible dominance of the direct $N-NO_2$ homolysis while the HONO isomerization still continues in the background, being the slower dissociation mechanism. The obtained conclusions are in excellent agreement with the earlier theoretical studies and the range of experimental data for the overall HMX decomposition.

Our calculations illustrate the importance of including the Arrhenius pre-factors in quantum chemical consideration of decomposition mechanisms of complex molecules. The HONO elimination and $N-NO_2$ homolysis have almost the same activation barriers and they would appear to be competing dissociation mechanisms in HMX. However, the reaction rate calculations show that the $N-NO_2$ fission in the triplet state is the 3 to 5 orders of magnitude faster reaction than the HONO elimination. This implies that the HONO elimination will play a minor role in the decomposition yielding the governing role to the $N-NO_2$ homolysis. This study and the performed analysis can be now extended to not only other materials but also to much more intricate solid state processes, which will facilitate the revelation of important details of extremely complex phenomena, such as the decomposition of condensed molecular materials and the behavior of materials under extreme conditions.

Acknowledgment. This work is supported in part by ONR Grant #N00014-09-1-0225 and by NSF Grant # DMR-100054. This research used resources of the NERSC, which is supported in part by the U.S. DoE under Contract No. DE-AC02-05CH11231. M.M.K. is grateful to the Office of the Director of National Science Foundation for support under the Independent Research and Development Program. Any appearance of findings, conclusions, or recommendations expressed in this material are those of the authors and do not necessarily reflect the views of NSF.

References and Notes

(1) Behrens, R. *J. Phys. Chem.* **1990**, *94*, 6706–6718.
(2) Behrens, R.; Bulusu, S. *J. Phys. Chem.* **1991**, *95*, 5838–5845.
(3) Brill, B. T.; Brush, P. G.; Kinloch, S. A.; Gray, P. *Philos. Trans. R. Soc. London, A: Math. Phys. Eng. Sci.* **1992**, *339*, 377–385.
(4) Chakraborty, D.; Muller, R. P.; Dasgupta, S.; Goddard, W. A., III. *J. Phys. Chem. A* **2001**, *105*, 1302–1314.
(5) Lewis, J. P.; Glaesemann, K. R.; VanOpdorp, K.; Voth, G. A. *J. Phys. Chem. A* **2000**, *104*, 11384–11389.
(6) Cobos, C. J. *J. Mol. Struct. (THEOCHEM)* **2005**, *714*, 147–152.
(7) Hanggi, P.; Talkner, P.; Borkovec, M. *Rev. Mod. Phys* **1990**, *62*, 251–341.
(8) Garret, B. C.; Truhlar, D. G. *J. Phys. Chem.* **1979**, *83*, 1052–1079.
(9) Sturdya, Y.; Claryb, D. C. *Phys. Chem. Chem. Phys.* **2007**, *9*, 2397–2405.
(10) Ashcroft, N. W.; Mermin, N. D. *Solid State Phys.* **1976**, 453.
(11) Wilson, A. H. *Thermodynamics and Statistical Mechanis*; Cambridge University Press: Cambridge, U.K., 1957; p 143.
(12) Hohenberg, P.; Kohn, W. *Phys. Rev.* **1964**, *136*, B864–B871.
(13) Kohn, W.; Sham, L. J. *Phys. Rev.* **1965**, *140*, A1133–A1138.

(14) Perdew, J. P.; Burke, K.; Ernzerhof, E. *Phys. Rev. Lett.* **1996**, *77*, 3865–3868.

(15) Blöchl, P. E. *Phys. Rev. B* **1994**, *50*, 17953–17979.

(16) Kresse, G.; Hafner, J. *Phys. Rev. B* **1993**, *47*, 558.

(17) Kresse, G.; Hafner, J. *Phys. Rev. B* **1994**, *49*, 14251.

(18) Kresse, G.; Furthmüller, J. *Comput. Mater. Sci.* **1996**, *6*, 15.

(19) Kresse, G.; Furthmüller, J. *Phys. Rev. B* **1996**, *54*, 11169–11186.

(20) Zhang, L.; Zybin, S. V.; van Duin, A. C. T.; Dasgupta, S.; Goddard, W. A., III. *J. Phys. Chem. A* **2009**, *113*, 10619–10640.

(21) Velardez, G. F.; Alavi, S.; Thompson, D. L. *J. Chem. Phys.* **2005**, *123*, 074313.

(22) Henkelman, G.; Uberuaga, B. P.; Jónsson, H. *J. Chem. Phys.* **2000**, *113*, 9901–9904.

(23) At the $N-NO_2$ distance exceeding 2.6 Å, the dissociated system prefers to stay in the triplet state as its total energy is lower than the singlet state's energy. We show here results of both as the singlet state dissociation vividly illustrates application of VTST. Sharia, O.; Kuklja, M. M. Modeling decomposition mechanisms in gaseous and crystalline cyclotetramethylene-tetranitramine, to be published.

(24) Assuming the error in the surface area at 100%, the absolute error in the rate constant would be 2 orders of magnitude smaller, 1.26%. The value of $\ln(A)$ for $N-NO_2$ is 47.6. Taking the surface area twice as large, $\ln(A)$ would become 48.2; hence the corresponding error in the rate constant would be $0.6/47.6 \times 100 = 1.26\%$.

(25) Baroni, S.; de Gironcoli, S.; Dal Corso, A. *Rev. Mod. Phys.* **2001**, *73*, 515–562.

(26) Goldstein, H. *Classical mechanics*; Addison-Wesley: Reading, MA, U.S., 1950; 399 pp.

(27) Zhang, S.; Nguyen, H. N.; Truong, T. N. *J. Phys. Chem. A* **2003**, *107*, 2981–2989, Our results can be compared with this work with caution, as α-HMX is simulated and a different methodology is used for calculations.

(28) Manaa, M. R.; Fried, L. E.; Melius, C. F.; Elstner, M.; Frauenheim, Th. *J. Phys. Chem. A* **2002**, *106* (39), 9024–9029, This study is performed for δ-HMX.

(29) Brill, T. B.; Gongwer, P. E.; Williams, G. K. *J. Phys. Chem.* **1994**, *98*, 12242–12247.

(30) Samoilenko, N. G.; Vinokurov, A. A.; Abramov, V. G.; Merzhanov, A. G. *Russ. J. Phys. Chem.* **1970**, *44*, 22–24.

(31) Campana, J. E.; Doyle, R. J., Jr. *J. Chem. Soc., Chem. Commun.* **1985**, 45–46.

(32) Zeman, S. *Thermochim. Acta* **1997**, *290*, 199–217.

(33) The experimental range is expected to be broader than the difference in the theoretical predictions because the clustering effect, catalysis, and secondary reactions will all effectively reduce the activation barriers measured. Variations in heating rates will also affect measurements.

JP108065C